PV Panel Heat Transfer Rate Enhancement Using a Novel Heat Exchanger with High-Resolution Spikes and Dimples

Mohammad E.Kashan[1*], *Alan s. Fung*[1], *John Swift*[2], and *Rakesh Kumar*[1]

[1]Toronto Metropolitan University (Former Ryerson), Centre for Sustainable Energy, Toronto, Canada.
[2]NUCAP Industries Inc. (Canada)

Abstract. PV cell electrical efficiency has an inverse relationship with its temperature. This study uses a novel and commercialized backsheet to reduce PV panel surface temperature. The novel backsheet consists of spikes and dimples to increase the air turbulence and convection heat transfer rate. Experimentally validated computational fluid dynamic (CFD) models are developed to investigate the influence of GripMetal backsheet on PV cell temperature and efficiency of PV panels and PVT collectors. Under 1000 W/m^2 solar irradiation, it is shown that a PVT collector with a 2.25 mm spikes height has almost 10% more electrical efficiency than a PVT collector with a flat plate channel. A maximum 22.5°C temperature drop was observed by using the GM-based PVT collector for slow-motion airflow. It is shown that the GM spikes are more efficient in low Reynolds numbers and can enhance air turbulence more effectively. The GM PVT collector has the best performance at low Reynolds numbers which is suitable for air-based PVT applications.

1 Introduction

Climate change catastrophes and energy crises are the most crucial concerns in the 21st century. Based on the IEEE report, global energy demands increased by 0.9% in 2019, equal to 120 million tons of oil equivalent. Decarbonisation efforts can be addressed using cleaner and more abundant energy sources such as solar energy. Photovoltaic and solar thermal collectors are the two favorite solar energy harvesting technologies. Different mechanisms cause PV efficiency reduction, such as recombination, reflection, absorption, dust and snow [1]. On the other hand, PV cell efficiency is inverse to the PV temperature. It has been shown that there is a 0.3%-0.5% PV power drop for each degree Celsius over the standard testing temperature (20°C) [2]. Furthermore, it was shown that thermal stress on the PV module due to the PV cell temperature elevation could reduce the whole PV module's lifetime [3]. To reduce the PV cell temperature, an efficient strategy of heat removal from the PV panel is necessary. Different passive and active methods are applied to control and reduce the PV cell temperature. Heat sinks and fins increase the surface area between the PV panel and the environment and enhance the convective heat transfer rate from the PV panel backsheet [4]. Elbreki et al. conducted a parametric and experimental study based on the attached lapping fins at the PV panel backsheet. It was shown that 18 fins with 20 cm height could make a 24.5°C temperature difference when compared to a reference PV panel of 0.35 m^2 [5]. Hybrid Photovoltaic-Thermal (PVT) collector consists of channels attached to the backshhet of the PV panel is one way to enhance the cooling of PV. By circulating fluid inside the channel, the thermal energy generated by the PV panel can be dissipated to the fluid and reduces the PV cell temperature. Rakesh and Rosen [6] performed a critical review of different air-based PVT collectors. The study showed the advantages of PVT collectors over regular PV panels in terms of PV panel efficiency, thermal energy production and space requirement. On the other hand, most of the studied PVT collectors are far from mass production and have complicated channel designs. The literature demonstrates considerable researches for PVT collectors and techniques to reduce the PV cell temperature. In most studies, fins and heat sinks have relatively large heights (10-25 cm) and thickness, which increases the production cost, the PV panel weight, and PV panel size [7], [8], [9].

This study uses a novel heat exchanger integrated in PV panels to evaluate the potential enhancement of PV cell temperature. The proposed heat exchanger (known as GRIPMetal), produced by NUCAP Industries Inc. GRIPMetal (GM) plates, consists of small spikes and dimples/cavities manufactured based on a unique skiving method which is simple, quick and cost-effective. GM spikes significantly increase surface area, breaking the laminar and thermal boundaries of fluid flow and enhancing fluid turbulence. GM spikes' surface enhancement make them an attractive opportunity to be used as heat exchanger on flat plates, inside the pipes or in other thermal applications. Spikes can be manufactured in a wide range of heights (0.58 mm to 3 mm), making them suitable for different applications and sizes.

Moreover, the novel skiving method is commercialized, and GM plates can be manufactured at a relatively low cost compared to other heat exchangers. Each spike is produced by removing part of the plate material that forms a dimple downstream of the spike. Thus, the skiving method creates an approximately equal volume of spikes and cavities on the surface of the plate. Fig. 1 shows a portion of a GM surface. Spike tip height is denoted by h, and the lateral distance between each spikes row is C_h. Table 1 shows the dimension of different GM plates with specific spike and groove

* Corresponding author: memamjome@ryerson.ca

dimensions.

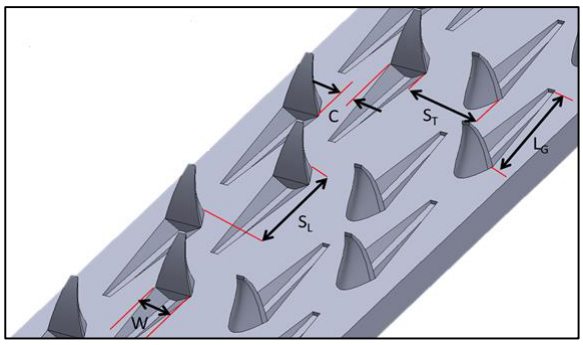

Fig. 1. GRIPMetal array overview.

Table 1. GM plates specifications

Hook Name	Hook Height (mm)	Hook Shape	Stream wise spacing (SL) (mm)	Span wise spacing (ST) (mm)	Width (mm)	Clearance (mm)
Heavy Duty	2.25	Straight	5.08	2.794	1.7272	0.127
Standard	1.52	Curved or Straight	3.175	2.286	1.016	0.381
Mini	1	Straight	2.54	1.0668	0.6096	0.6096
Nano	0.63	Straight	1.905	0.5842	0.2794	0.2794

2 System description

The primary scope of this study is to evaluate the effect of GM plates on PV cell temperature and efficiency. Two scenarios are proposed to enhance heat dissipation from the PV cell to the surrounding. In a Photovoltaic panel, PV cells are encapsulated between transparent EVA layers. EVA layer has a low conduction coefficient that reduces heat dissipation from the PV cell to the surrounding. In the first part of this study, the GM plate is used as the backsheet, and its spikes penetrated the bottom EVA layer. The potential EVA layer conduction coefficient enhancement is studied, and constraints are evaluated. In the second part, the GM plate is used as a heat exchanger inside the channel of an air-based PVT collector. The limitation of using GM heat exchangers in the PVT collector and PV cell temperature enhancement is studied.

2.1 Evaluation of EVA layer Thermal Conductivity Enhancement by Penetrating GM spikes to the EVA layer

A PV cell is encapsulated between EVA layers to protect the PV cell from physical damage and electrical leakage. Due to the low thermal conductivity of the EVA layer, the thermal energy generated in the PV cell cannot be dissipated efficiently from the PV cell to the surrounding. In the first part of the study, the GM plate is used to study the potential enhancement of the EVA layer's thermal conductivity and PV cell temperature and efficiency. The GM plate is used as the back sheet, and the spikes of the GM plate are penetrated the lower EVA layer to increase the total thermal conductivity of the EVA layer (Fig. 2.b). The GM plate has 0.5 mm thickness and is made of aluminum. The shortest and longest spike height are 0.63mm and 2.25mm respectively. Table 2 shows the material specification of a PV cell [10]. The PV cell is 10cm × 10cm, and 800 W/m^2 heat generation on the PV cell surface is considered. The top and bottom surfaces of the PV cell are exposed to 1 m/s air flow at 25 ℃ temperature. All the other sides of the PV cell are considered adiabatic surfaces. Two methods are used to calculate the PV cell temperature. Analytical analysis and Computational Fluid Dynamic (CFD) models are presented and compared to evaluate the EVA heat conduction enhancement. The CFD model is designed in COMSOL Multiphysics software.

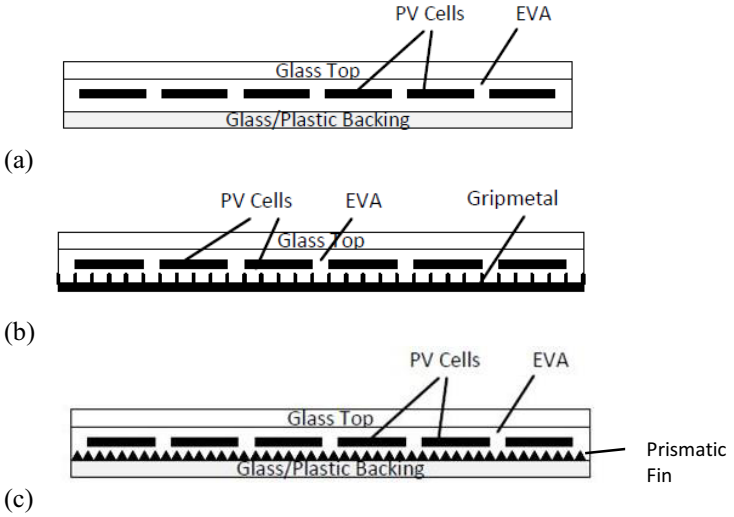

Fig. 2. (a). Conventional PV cell schematic. (b). PV panel with GM back sheet. GM spikes are penetrated into the bottom EVA layer. (c). Hypothetical prismatic fins penetrated into the EVA layer.

Table 2. PV cell layers' specification [10].

Layer	Layer Thickness (m)	Thermal Conductivity (W/K.m)
Glass	0.003	0.98
EVA	0.0004	0.23
Solar Cell	0.00018	148
EVA (Bottom)	0.0004	0.23
Aluminum Backsheet	0.0005	155

2.1.1 Analytical Equations and Results

Fig. 3 shows the thermal resistance schematic of a PV panel with e_g energy generation inside the PV cell. The energy generation is due to solar irradiation that is

converted to heat inside the PV cell. The PV cell is assumed to be an isothermal layer due to having a thin thickness and high thermal conductivity. The radiation from PV cells is neglected. In Equation 1, R_{T1} is the equivalent thermal resistance of the PV panel's top part which consists of top EVA layer, glass, and convection heat transfer between the glass layer and air. In equation 2, R_{T2} is the equivalent thermal resistance of the PV panel's bottom part which consists of bottom EVA layer, the backsheet, and convection heat transfer between the backsheet layer and air. l_g, l_{EVA1}, l_{EVA2} and l_b are the thickness of the glass, top EVA layer, bottom EVA layer and backsheet layer, respectively. The convective heat transfer coefficient on the glass and the backsheet side are assumed to equal h. Glass, backsheet, and EVA thermal conductivity are shown by k_g, k_b, and k_{EVA}. Considering an energy balance for the PV node, the PV cell temperature (T_{PV}) can be calculated from Equation 1. The radiation from the PV cell to the atmosphere is neglected for the simplification of the problem.

$$T_{PV}=e_g l\left(\frac{R_{T1}R_{T2}}{R_{T1}+R_{T2}}\right)+T_\infty \quad (1)$$

$$R_{T1}=\frac{1}{h}+\frac{l_g}{k_g}+\frac{l_{EVA1}}{k_{EVA}} \quad (2)$$

$$R_{T2}=\frac{1}{h}+\frac{l_b}{k_b}+\frac{l_{EVA2}}{k_{EVA}} \quad (3)$$

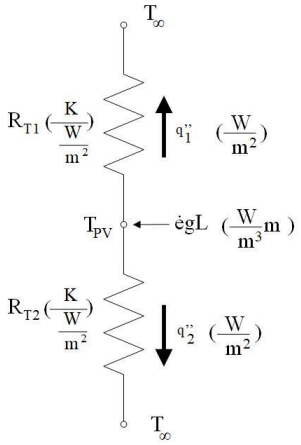

Fig. 3. Thermal resistance equivalent of a PV panel.

CFD simulations and analytical calculations for a typical PV panel with an aluminum and Tedlar backsheet show 54.08°C and 54.37°C PV cell temperature, respectively. The analytical and CFD model results are in good agreement and have less than a 1% difference. An extreme scenario is introduced to estimate the maximum possible PV cell temperature drop due to using spikes or material penetrated the EVA layer. It is assumed that an aluminum layer with a thickness equal to the GM spike height is replaced with a portion of the EVA layer. In other words, it is assumed that the average thickness of the EVA layer is reduced, which is equal to the GM spike height, and the backsheet layer thickness is increased, equivalent to the GM spike height (Extreme scenario). Another simplified model considers rectangular prism fins instead of GM spikes, penetrating the EVA layer. This configuration has a much higher aluminum concentration inside the EVA layer than the GM spikes. Thus the prismatic fins must have a more significant temperature drop than GM spikes due to having more aluminum concentration. Table 3 shows the result of all the introduced scenarios with different patterns and spike sizes. Since the mini spike height is bigger than the EVA layer thickness, two or three EVA layers are needed for the PV panel's lower part to cover the spikes fully. It is shown that the lowest PV temperature is for the extreme Nano size scenario with 53.88°C, which is 0.2°C less than the conventional PV panel with one layer of EVA. If the extreme case is replaced with the actual GM plate, the thermal conductivity will drop, and the PV cell temperature will be higher than in the extreme scenario. For example, for Prismatic Nano fin inside the EVA layer, the PV temperature is 0.6°C higher than the conventional PV panel which is undesirable.

Table 3. PV cell temperature for different EVA layer scenarios.

	Scenario	PV Cell Temperature (°C)	EVA Thickness (mm)
Conventional PV panel	Conventional PV panel/One EVA layer/Tedlar backsheet	54.37	0.4
	Conventional PV panel/One EVA layer/Al backsheet	54.08	0.4
	Conventional PV panel/Two EVA layer/Aluminum	54.44	0.8
	Conventional PV panel/Three EVA layer	54.79	1.2
Extreme Scenario-Analytical	Extreme-Nano Thickness-Two EVA Layer	53.88	0.17
	Extreme-Nano Thickness-Three EVA Layer	54.24	0.57
	Extreme-Mini Thickness-Three EVA Layer	53.9	0.2
COMSOL Model/ Conic Spikes	Prismatic Mini size fin inside the EVA-Three EVA layer	54.68	1.2
	Prismatic Nano fin inside the EVA-Three EVA layer	54.72	1.2

Based on the analytical and CFD models, it is observed that the penetration of the GM's spikes into the EVA layers has minimal heat transfer enhancement for the PV cell when there is no convective heat transfer enhancement around the PV module. This finding agrees with experimental work of Harb et al.[11] on influence of EVA layer on the PV temperature. They found that by reducing the lower EVA layer thickness from 1mm to 0.2 mm, the PV cell temperature reduces slightly from 51.8°C to 51°C. In their study, the EVA layer thickness is reduced by a factor of 5 and the temperature reduction is 0.7°C. In the current study for the hypothetical case that there is very thin EVA layer (0.17 mm), a 0.2°C temperature reduction was observed. On the other hand, Harb et al. [11] concluded that EVA thickness substantially influences the PV cell temperature for concentrated PV panels when much higher solar irradiation is applied to the panel. At a Concentration Ratio (CR) of 30 they could achieve 51°C temperature reduction by reducing the EVA thickness from 1mm to 0.2mm. This finding agrees with current analytical and COMSOL models. The EVA

characteristics can influence the heat transfer at very high solar irradiation (CR=20 or more) and high backsheet heat transfer coefficient with air or liquid coolant. This case is not applicable to the current case study of regular PV or PVT panels. It can be concluded that GM spikes have minimal enhancement on the PV cell temperature for a concentration ratio of 1 to 5. But it can be studied for higher CRs. And also, the possibility of electricity leakage through the GM spikes should be considered for the system design because of the spikes' penetration to the EVA layer.

2.2 Air-Based PVT Heat Transfer Enhancement by Means of GM Plates

In air-based PVT collectors, forced convection dissipates generated heat by the PV cell more effectively than natural convection in PV panels. In addition, the dissipated heat can be used as a heat source for different applications like air source heat pumps. By enhancing the heat exchange rate from the PV cells to the PVT air channel, the electrical and thermal efficiency of the PVT collector can be enhanced. In the second part of the study, the GM plate will be used as the heat exchanger inside the air channel to enhance the heat exchange rate compared with a flat plate channel.

2.2.1 System Description-Part Two

The GM plate can improve the heat exchange rate in two ways: a) increasing the surface area using high-resolution spikes and dimples and b) breaking the flow and thermal boundary layers and increasing the fluid turbulence. Fig. 4 shows the schematic of an air-based PVT with GM plates on two sides of the air channel. To study the potential enhancement of the convection heat transfer coefficient of the channel, a CFD model of the PVT collector is created in COMSOL Multiphysics software. The GM plate consists of tiny spikes and dimples with a complex curved geometry that makes the simulation costly in terms of simulation time and computational hardware. To reduce the computational cost, the convection heat transfer coefficient of GM plates is derived from the experiments carried by [12]. In this study, a channel that consists of GM plates on the top and bottom is fabricated. Different GM spike sizes and channel heights are tested to find GM plates' convection heat transfer coefficient. Correlations for different Re numbers and channel heights are derived from the experimental data. Considering the experimental results for the air channel, a GM channel model in COMSOL software is created and calibrated for sensitivity analysis. All the boundary conditions and geometry dimensions are taken from the experimental setup to have a model the same as the tested setup. Fig. 5 shows that the convection heat transfer coefficient calculated by the CFD model is in agreement with the experimental results. Thus the CFD model of the GM channel can be used for further sensitivity analysis.

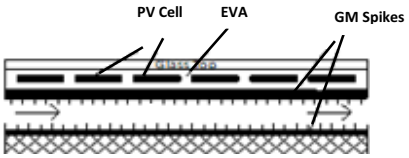

Fig. 4. Air-based PVT with double sided GM channel.

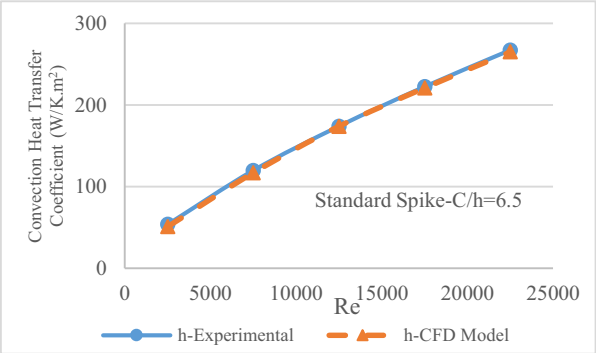

Fig. 5. Convection heat transfer coefficient calculated from the CFD model and experimental tests for standard spike size and C/h=6.5.

Based on the calibrated CFD model for the GM channel, a PVT collector is modelled in COMSOL, which consists of a double-sided GM channel attached to the back side of a PV panel. Airflow with different velocities, using a fan passing through the channel, and dissipates the generated heat inside the PV cells. Air leaves the PVT from onside and fresh air comes in from the inlet. The specification of the PV panel is the same as in the first part of the study. The PV has 17.51% reference efficiency and its temperature coefficient is β=0.394 (%/°C) at a reference temperature of 20°C, which means that for each degree Celsius increase in temperature, there is a 0.394% PV efficiency drop. Fig. 6 shows the mesh independency of the CFD model for one sample case of PVT collector. It is shown that the CFD model with 208168 nodes can be considered as the optimum mesh size for the model since the PV temperature difference is less than 1% of finer mesh size.

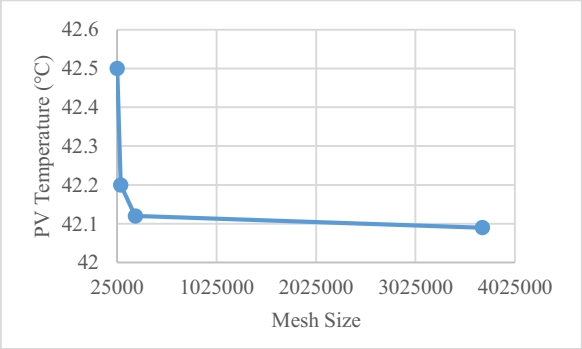

Fig. 6. PVT model mesh independency diagram.

2.2.2 PVT collector simulation results

For the first scenario (Case A), three different C/h numbers (channel height to spike size) are considered to study the influence of GM plates geometry on the PV cell temperature. For each C/h, different Reynolds

numbers are considered to evaluate the influence of spike height, channel height and airflow velocity on the PV cell temperature. Equation 4 defines Re number which V_{air} is the wind air speed inside the channel, ρ is the air density and μ is air dynamic viscosity. Hydraulic diameter (D_h) for a flat plate channel is calculated from Equation 5.

$$Re = \frac{V_{air} \times D_h \times \rho}{\mu} \quad (4)$$

$$D_h = \frac{2(channel\ height \times channel\ width)}{channel\ height + channel\ width} \quad (5)$$

A reference PVT collector with a flat plate channel is modelled (Case B) to be compared with Case A results.

Fig. 7 shows the PV cell temperature difference between Case A and Case B for different C/h and Re numbers. It is shown that in all conditions, Case A, which has a GM air channel, has a lower PV temperature than Case B, which has a flat plate channel. The temperature difference gradually decreases and can be considered unchangeable for high Re numbers. The maximum temperature difference occurs on low Re numbers, semi laminar fluid, which means lower air velocity for a specific channel geometry. The effect of GM spikes on the heat exchange rate in low Re numbers is significantly higher than in higher Re numbers. In low Re numbers, GM plates can increase air turbulence, and heat transfer rate. Therefore, higher temperature drops can be achieved in GM channel. On the other hand, for high Re numbers, both Cases A and B have a similar fluid mix which causes a minimal temperature difference between them. The maximum temperature drops of 22.5°C and 21.3°C are for C/h=4.5 and C/h=6.5, which has heavy-duty spike size on the surface of the GM.

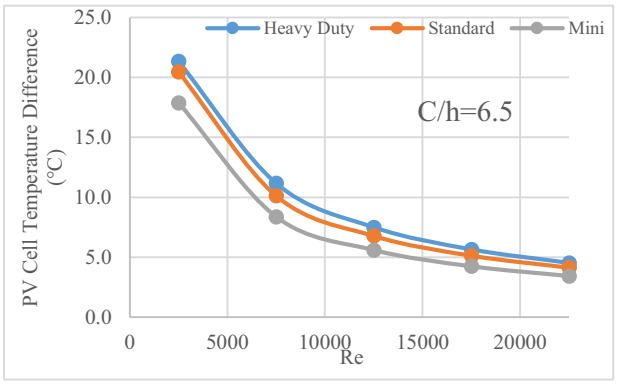

(a)

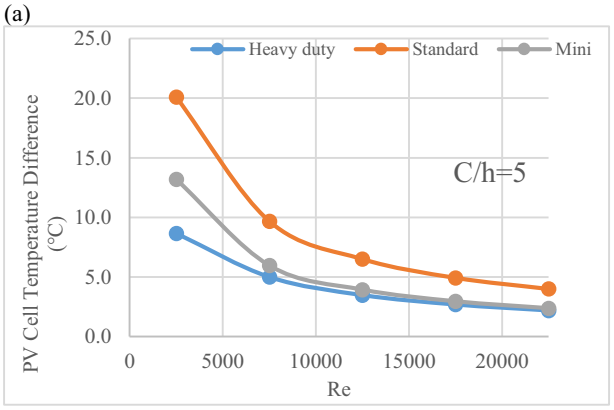

(b)

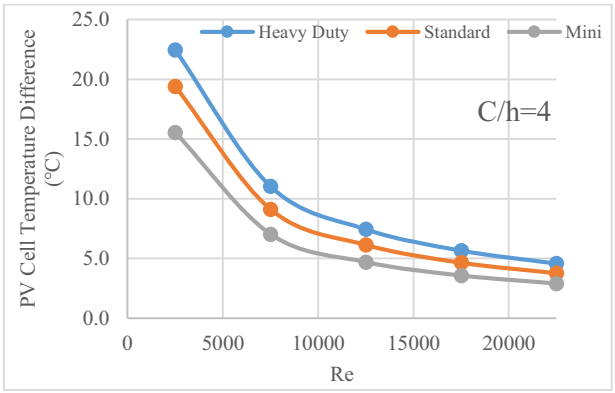

(c)

Fig. 7. PV cell temperature difference between Case A and B. a) C/h=6.5, b) C/h=5, c) C/h=4

Because of the lower PV cell temperature in Case A, the PV panel efficiency is enhanced compared to Case B. Fig. 8 shows the maximum 10.4% and 10.14% efficiency enhancement at Re=2500 for C/h=4.5 and C/h=6.5 which heavy-duty spike size is used on the surface of the GM. This means that the combination of low Re numbers, slow motion air flow, and big spikes have the highest PV cell efficiency enhancement among other scenarios.

The better efficiency enhancement of heavy-duty spikes is due to the more significant effect of spikes on the thermal boundary layer close to the wall and increasing the fluid turbulence. Lower Re number and air flow rate are more applicable in PVT collectors. Thus, the GM air channel can be an excellent fit for an air-based PVT collector. Since GM technology is well-developed, the manufacturing cost has been reduced, and there is no noticeable production cost difference between a flat plate PVT and the GM PVT collector. On the other hand, for the GM PVT collector, the PV cell efficiency can be more than 10% of that of a flat plate collector.

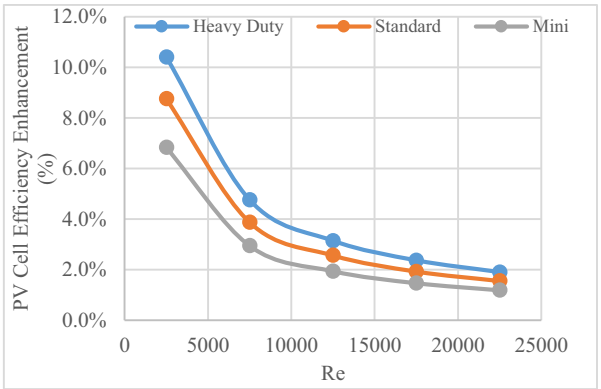

(a)

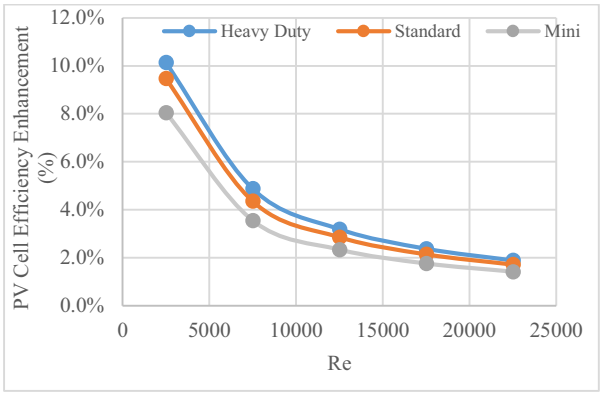

(b)

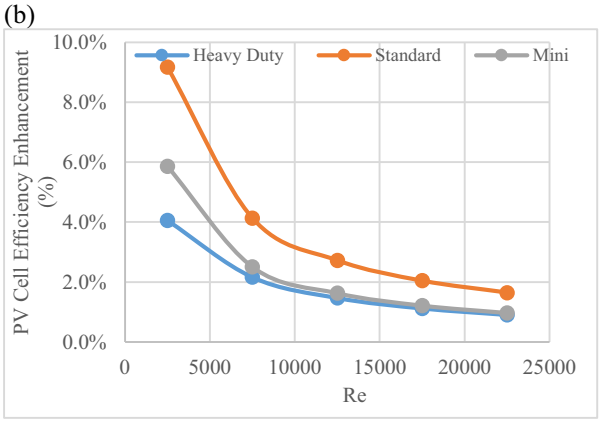

(c)

Fig. 8. PV panel electrical efficiency difference between Case A and B. a) C/h=6.5, b) C/h=5, c) C/h=4

3 Conclusion and Future Work

In the current study, a novel heat exchanger named GRIPMetal (GM) plate is used to investigate the potentials of PV panel cooling effectiveness and electrical efficiency enhancement. The outcome of the study can be concluded as below:

- For the first part of the study, the GM spikes are assumed to have penetrated the solar cells' bottom EVA layer to study potential heat transfer enhancement. It is shown that penetrating the GM spikes has minimal heat transfer enhancement, and the PV cell temperature is not reduced effectively. On the other hand, there is a potential electrical leakage if the GM spikes penetrate the EVA layer. Adding more EVA layers to eliminate the electrical leakage probability can increase the PV cell temperature, which is undesirable.
- For the second part of the study, the GM heat exchanger is used on both sides of an air-based PVT collector to increase the convection heat transfer coefficient. A COMSOL model for the PVT collector is created based on the reported experimental results of the GRIPMetal to study the PV cell temperature. It is shown that for different channel heights and Re numbers, the collector with GM air channel (Case A) has a lower PV cell temperature than a flat plate PVT collector (Case B).
- The maximum temperature drops of 22.5°C and 21.3°C are for C/h=4.5 and C/h=6.5, which have heavy duty spike size on the surface of the GM.
- By increasing the Re number, the influence of GM on the PV cell temperature drop reduces significantly. It was shown that the GM channel is beneficial in low Re numbers, for all the C/h numbers, with low-velocity airflow inside the channel.
- In low Re numbers, the GM spikes significantly increase the airflow mix and enhance the heat transfer rate.
- At high Re numbers (Re>15000), the influence of the GM spikes is minimal on the heat transfer augmentation. Due to high inlet air velocity, both Cases A and B have full mixed fluid with no thermal boundary layer. Thus the influence of the GM spikes on the heat transfer rate is minimal at high Re numbers.
- Low Re numbers are the best fit for PVT applications due to lower airflow velocity and lower pressure drop and related fan energy consumption.
- In this work, the studied channels height is varied between 0.5 cm to almost 2 cm. The narrow channel can increase the pressure drop, and a bigger fan is needed. Future work will expand the CFD model for bigger channel heights. Also, the pressure drop can be calculated to find an optimum design for the PVT channel.

References

[1] W. Shockley and H. J. Queisser, "Detailed Balance Limit of Efficiency of p-n Junction Solar Cells," *J. Appl. Phys.*, vol. 32, no. 3, pp. 510–519, 1961, doi: 10.1063/1.1736034.

[2] E. Skoplaki and J. A. Palyvos, "On the temperature dependence of photovoltaic module electrical performance: A review of efficiency/power correlations," *Sol. Energy*, vol. 83, no. 5, pp. 614–624, 2009, doi: 10.1016/j.solener.2008.10.008.

[3] A. Ndiaye, C. M. F. Kébé, A. Charki, P. A. Ndiaye, V. Sambou, and A. Kobi, "Degradation evaluation of crystalline-silicon photovoltaic modules after a few operation years in a tropical environment," *Sol. Energy*, vol. 103, pp. 70–77, May 2014, doi: 10.1016/j.solener.2014.02.006.

[4] P. N, L. Pandiyan, N. G, A. S, and V. V, "Experimental analysis on passive cooling of flat photovoltaic panel with heat sink and wick structure," *Energy Sources Part Recovery Util. Environ. Eff.*, vol. 42, no. 6, pp. 653–663, 2020, doi: 10.1080/15567036.2019.1588429.

[5] S. V. Hudișteanu, F. E. Țurcanu, N. C. Cherecheș, C. G. Popovici, M. Verdeș, and I. Huditeanu, "Enhancement of PV Panel Power Production by Passive Cooling Using Heat Sinks with Perforated Fins," *Appl. Sci.*, vol. 11, no. 23, p. 11323, 2021, doi: 10.3390/app112311323.

[6] R. Kumar and M. A. Rosen, "A critical review of photovoltaic–thermal solar collectors for air heating," *Appl. Energy*, vol. 88, no. 11, pp. 3603–3614, 2011, doi: 10.1016/j.apenergy.2011.04.044.
[7] C. G. Popovici, S. V. Hudişteanu, T. D. Mateescu, and N.-C. Cherecheş, "Efficiency Improvement of Photovoltaic Panels by Using Air Cooled Heat Sinks," *Energy Procedia*, vol. 85, no. Journal Article, pp. 425–432, 2016, doi: 10.1016/j.egypro.2015.12.223.
[8] Z. Zou, W. Yan, H. Gong, Y. Wang, and J. Shao, "Quantifying the performance advantage of the novel passive air cooling system for PV array and system structure optimization," *Appl. Therm. Eng.*, vol. 149, no. Journal Article, pp. 899–908, 2019, doi: 10.1016/j.applthermaleng.2018.12.085.
[9] S. Nižetić, A. M. Papadopoulos, and E. Giama, "Comprehensive analysis and general economic-environmental evaluation of cooling techniques for photovoltaic panels, Part I: Passive cooling techniques," *Energy Convers. Manag.*, vol. 149, no. Journal Article, pp. 334–354, 2017, doi: 10.1016/j.enconman.2017.07.022.
[10] J. Allan, H. Pinder, and Z. Dehouche, "Enhancing the thermal conductivity of ethylene-vinyl acetate (EVA) in a photovoltaic thermal collector," *AIP Adv.*, vol. 6, no. 3, pp. 35011-035011–9, 2016, doi: 10.1063/1.4944557.
[11] A. E.-M. A. Harb, A. Radwan, K. Elsayed, M. Sedrak, and M. Ahmed, "Influence of varying the Ethylene-Vinyl Acetate layer thicknesses on the performance of a polycrystalline silicon solar cell integrated with a microchannel heat sink," *Sol. Energy*, vol. 195, no. Journal Article, pp. 592–609, 2020, doi: 10.1016/j.solener.2019.11.082.
[12] O. Khaled, J. Swift, and R. Kempers, "Thermal enhancement of rectangular channels using hook-shaped fins and dimples," *Appl. Therm. Eng.*, vol. 217, no. Journal Article, 2022, doi: 10.1016/j.applthermaleng.2022.119272.